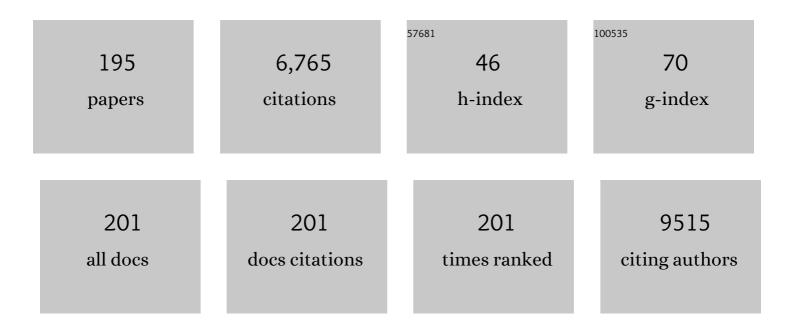


List of Publications by Year in descending order

Source: https://exaly.com/author-pdf/6291137/publications.pdf Version: 2024-02-01



FENC YU

#	Article	lF	CITATIONS
1	Enhanced oxygen reduction reaction performance of Co@N–C derived from metal-organic frameworks ZIF-67 via a continuous microchannel reactor. Chinese Chemical Letters, 2023, 34, 107128.	4.8	7
2	Robust photo-assisted removal of NO at room temperature: Experimental and density functional theory calculation with optical carrier. Green Energy and Environment, 2023, 8, 1102-1116.	4.7	2
3	Ni-Al mixed metal oxide with rich oxygen vacancies: CO methanation performance and density functional theory study. Chinese Journal of Chemical Engineering, 2022, 46, 73-83.	1.7	1
4	Fabrication of surface oxygen vacancies on NiMnAl-LDO catalyst by high-shear mixer-assisted preparation for low-temperature CO2 methanation. Fuel, 2022, 309, 122099.	3.4	14
5	3D Cross-linked Ti3C2Tx-Ca-SA films with expanded Ti3C2Tx interlayer spacing as freestanding electrode for all-solid-state flexible pseudocapacitor. Journal of Colloid and Interface Science, 2022, 610, 295-303.	5.0	11
6	Construction of graphitic-N-rich TiO2-N-C interfaces via dye dissociation and reassembly for efficient oxygen evolution reaction. Chemical Engineering Journal, 2022, 431, 133246.	6.6	11
7	Visible-light-activated TiO2–NiFe2O4 heterojunction for detecting sub-ppm trimethylamine. Journal of Alloys and Compounds, 2022, 898, 162990.	2.8	9
8	Enhanced carbon dioxide capture performance of natural mineral vermiculiteâ€derived lithium silicate with Na doping. , 2022, 12, 263-272.		2
9	Photoâ€Assisted CO/CO ₂ Methanation over Ni/TiO ₂ Catalyst: Experiment and Density Functional Theory Calculation. ChemCatChem, 2022, 14, .	1.8	3
10	CuCeO _{<i>x</i>} /VMT powder and monolithic catalyst for CO-selective catalytic reduction of NO with CO. New Journal of Chemistry, 2022, 46, 10422-10432.	1.4	2
11	Enhanced photoelectrochemical performance of ZnO/NiFe-layered double hydroxide for water splitting: Experimental and photo-assisted density functional theory calculations. Journal of Colloid and Interface Science, 2022, 623, 285-293.	5.0	9
12	Facile Synthesis of Metal–Organic Framework ZIF-67 via a Multi-Inlet Vortex Mixer Using Various Solvents: MeOH, EtOH, H ₂ O, and Baijiu. Industrial & Engineering Chemistry Research, 2022, 61, 7952-7961.	1.8	4
13	Enhanced low-temperature CO-SCR denitration performance and mechanism of two-dimensional CuCoAl layered double oxide. Journal of Environmental Chemical Engineering, 2022, 10, 108030.	3.3	13
14	Confined Jet Impingement Continuous Microchannel Reactor Synthesis of Ultrahigh-Quality Mesoporous Silica Nanospheres for CO ₂ Capture. Industrial & Engineering Chemistry Research, 2022, 61, 9300-9310.	1.8	2
15	La-enhanced Ni nanoparticles highly dispersed on SiC for low-temperature CO methanation performance. Rare Metals, 2021, 40, 1753-1761.	3.6	5
16	Cobalt substituted polyoxophosphomolybdate modified TiO2 for boosted photoelectrocatalytic water oxidation. Journal of Alloys and Compounds, 2021, 854, 157232.	2.8	8
17	CO2 conversion in a coaxial dielectric barrier discharge plasma reactor in the presence of mixed ZrO2-CeO2. Journal of Environmental Chemical Engineering, 2021, 9, 104654.	3.3	16
18	Directly application of bimetallic 2D-MOF for advanced electrocatalytic oxygen evolution. International Journal of Hydrogen Energy, 2021, 46, 416-424.	3.8	30

#	Article	IF	CITATIONS
19	Self-synergistic cobalt catalysts with symbiotic metal single-atoms and nanoparticles for efficient oxygen reduction. Journal of Materials Chemistry A, 2021, 9, 1127-1133.	5.2	21
20	NaKB ₆ O ₉ F ₂ : a new complex alkali metal fluorooxoborate with puckered layers. New Journal of Chemistry, 2021, 45, 2974-2980.	1.4	7
21	Multifunctional book-like CuCo-MOF for highly sensitive glucose detection and electrocatalytic oxygen evolution. New Journal of Chemistry, 2021, 45, 16714-16721.	1.4	21
22	Na ₂ La ₂ B ₁₀ O ₁₉ : a new lanthanum sodium borate with infinite 2D layer 2â^ž[B ₁₀ O ₁₉] ^{8â^^} and moderate birefringence. New Journal of Chemistry, 2021, 45, 13592-13598.	1.4	4
23	A new acentric borate–nitrate Cs ₃ B ₈ O ₁₃ (NO ₃) with interpenetrating porous 3D covalent and ionic lattices. Dalton Transactions, 2021, 50, 8676-8679.	1.6	4
24	Three-dimensional porous Mn–Ni/Al2O3 microspheres for enhanced low temperature CO hydrogenation to produce methane. International Journal of Hydrogen Energy, 2021, 46, 7912-7925.	3.8	6
25	Review of ZnO-based nanomaterials in gas sensors. Solid State Ionics, 2021, 360, 115544.	1.3	211
26	A review of biomass-derived graphene and graphene-like carbons for electrochemical energy storage and conversion. New Carbon Materials, 2021, 36, 350-372.	2.9	29
27	Reducing N ₂ O Formation over COâ€SCR Systems with CuCe Mixed Metal Oxides. ChemCatChem, 2021, 13, 2709-2718.	1.8	32
28	Enhanced low-temperature CO/CO2 methanation performance of Ni/Al2O3 microspheres prepared by the spray drying method combined with high shear mixer-assisted coprecipitation. Fuel, 2021, 291, 120127.	3.4	11
29	Ethanol Sensing Properties and First Principles Study of Au Supported on Mesoporous ZnO Derived from Metal Organic Framework ZIF-8. Sensors, 2021, 21, 4352.	2.1	12
30	Active sites engineering via tuning configuration between graphitic-N and thiophenic-S dopants in one-step synthesized graphene nanosheets for efficient water-cycled electrocatalysis. Chemical Engineering Journal, 2021, 416, 129096.	6.6	27
31	Understanding the CO2 chemical reaction path on Li6ZnO4, a new possible high temperature CO2 captor. Chemical Engineering Journal, 2021, 417, 129205.	6.6	14
32	3D-printed monolithic catalyst of Mn-Ce-Fe/attapulgite for selective catalytic reduction of nitric oxide with ammonia at low temperature. Journal of Environmental Chemical Engineering, 2021, 9, 105753.	3.3	9
33	Modification of NiFe layered double hydroxide by lanthanum doping for boosting water splitting. Electrochimica Acta, 2021, 390, 138824.	2.6	30
34	The Effect of Mass Transfer Rate-Time in Bubbles on Removal of Azoxystrobin in Water by Micro-Sized Jet Array Discharge. Catalysts, 2021, 11, 1169.	1.6	3
35	Ultralow specific surface area vermiculite supporting Mn-Ce-Fe mixed oxides as "curling catalysts― for selective catalytic reduction of NO with NH3. Green Chemical Engineering, 2021, 2, 284-293.	3.3	10
36	Two-dimensional vermiculite carried CuCoCe catalysts for CO-SCR in the presence of O2 and H2O: Experimental and DFT calculation. Chemical Engineering Journal, 2021, 422, 130099.	6.6	48

#	Article	IF	CITATIONS
37	Revealing the active sites of the structured Ni-based catalysts for one-step CO2/CH4 conversion into oxygenates by plasma-catalysis. Journal of CO2 Utilization, 2021, 52, 101675.	3.3	24
38	Transition-metalâ€doped ceria carried on two-dimensional vermiculite for selective catalytic reduction of NO with CO: Experiments and density functional theory. Applied Surface Science, 2021, 566, 150704.	3.1	21
39	Two-dimensional layered double hydroxides as a platform for electrocatalytic oxygen evolution. Journal of Materials Chemistry A, 2021, 9, 9389-9430.	5.2	83
40	Robust Artificial Solidâ€Electrolyte Interfaces with Biomimetic Ionic Channels for Dendriteâ€Free Li Metal Anodes. Advanced Energy Materials, 2021, 11, 2003496.	10.2	64
41	Light-Excited Ag-Doped TiO2â ``CoFe2O4 Heterojunction Applied to Toluene Gas Detection. Nanomaterials, 2021, 11, 3261.	1.9	3
42	The influence of Pt loading and dispersion on the NOx storage and reduction performance of Pt/K2CO3/Co1Mg2Al1Ox catalysts. Catalysis Today, 2020, 339, 148-158.	2.2	11
43	Overwhelming electrochemical oxygen reduction reaction of zinc-nitrogen-carbon from biomass resource chitosan via a facile carbon bath method. Chinese Chemical Letters, 2020, 31, 1207-1212.	4.8	13
44	Walnut shell-derived hierarchical porous carbon with high performances for electrocatalytic hydrogen evolution and symmetry supercapacitors. International Journal of Hydrogen Energy, 2020, 45, 443-451.	3.8	55
45	Zinc and Nitrogen-Doped Carbon In-Situ Wrapped ZnO Nanoparticles as a High-Activity Catalyst for Acetylene Acetoxylation. Catalysis Letters, 2020, 150, 1155-1162.	1.4	12
46	K _{2.64} Cs _{0.36} SiF ₇ : a new fluorosilicate with a <i>trans</i> -perovskite structure. New Journal of Chemistry, 2020, 44, 2727-2732.	1.4	3
47	Polyoxometalate intercalated NiFe layered double hydroxides for advanced water oxidation. International Journal of Hydrogen Energy, 2020, 45, 1802-1809.	3.8	37
48	3D Model of an Order-Structured Cathode Catalyst Layer with Vertically Aligned Carbon Nanotubes for PEM Fuel Cells under the Water Flooding Condition. ACS Sustainable Chemistry and Engineering, 2020, 8, 695-705.	3.2	9
49	Up-scaled synthesis of flower-like SiO2 microspheres via continuous flash nanoprecipitation and their application as a catalyst support. Energy Reports, 2020, 6, 2724-2734.	2.5	0
50	Combustion Products of Calcium Carbide Reused by Cu-Based Catalysts for Acetylene Carbonylation. ACS Omega, 2020, 5, 27692-27701.	1.6	3
51	Improved oxygen reduction performance of a N, S co-doped graphene-like carbon prepared by a simple carbon bath method. New Carbon Materials, 2020, 35, 531-539.	2.9	15
52	Synthesis of Co2â^'xNixO2 (0 < x < 1.0) hexagonal nanostructures as efficient bifunctional electrocatalysts for overall water splitting. Dalton Transactions, 2020, 49, 6587-6595.	1.6	20
53	New Catalytic and Sorption Bifunctional Li ₆ CoO ₄ Material for Carbon Monoxide Oxidation and Subsequent Chemisorption. Industrial & Engineering Chemistry Research, 2020, 59, 10823-10831.	1.8	6
54	A facile approach to synthesize CoO-Co3O4/TiO2 NAs for reinforced photoelectrocatalytic water oxidation. Journal of Solid State Electrochemistry, 2020, 24, 941-950.	1.2	4

#	Article	IF	CITATIONS
55	In situ molecular-level synthesis of N, S co-doped carbon as efficient metal-free oxygen redox electrocatalysts for rechargeable Zn–Air batteries. Applied Materials Today, 2020, 20, 100737.	2.3	22
56	Revealing the dependence of active site configuration of N doped and N, S-co-doped carbon nanospheres on six-membered heterocyclic precursors for oxygen reduction reaction. Journal of Catalysis, 2020, 389, 677-689.	3.1	33
57	Plasma for Energy and Catalytic Nanomaterials. Nanomaterials, 2020, 10, 333.	1.9	4
58	Two-dimensional MnFeCo layered double oxide as catalyst for enhanced selective catalytic reduction of NOx with NH3 at low temperature (25–150 °C). Applied Catalysis A: General, 2020, 592, 117432.	2.2	25
59	Enhanced selective catalytic reduction of NO with CO over Cu/C nanoparticles synthetized from a Cu-benzene-1,3,5-tricarboxylate metal organic framework by a continuous spray drying process. Chemical Engineering Journal, 2020, 388, 124270.	6.6	25
60	Overwhelming low ammonia escape and low temperature denitration efficiency via MnO -decorated two-dimensional MgAl layered double oxides. Chinese Journal of Chemical Engineering, 2020, 28, 1925-1934.	1.7	5
61	Uniformly dispersed Fe3C (~5 nm) in Fe-N-doped carbon nanosheets derived from coal tar pitch as efficient electrocatalysts for oxygen reduction reaction. Materials Letters, 2020, 273, 127861.	1.3	7
62	Preparation of highly dispersed supported Ni-Based catalysts and their catalytic performance in low temperature for CO methanation. Carbon Resources Conversion, 2020, 3, 164-172.	3.2	4
63	Fe ₃ O ₄ /Fe ₃ C@Nitrogenâ€Doped Carbon for Enhancing Oxygen Reduction Reaction. ChemNanoMat, 2019, 5, 187-193.	1.5	15
64	Naphthalene-modulated microporous carbon layers of LiFePO4 improve the high-rate electrochemical performance. Journal of Energy Chemistry, 2019, 30, 84-89.	7.1	8
65	A review of recent advances in two-dimensional natural clay vermiculite-based nanomaterials. Materials Research Express, 2019, 6, 102002.	0.8	31
66	Flocculant-Assisted Synthesis of Graphene-Like Carbon Nanosheets for Oxygen Reduction Reaction and Supercapacitor. Nanomaterials, 2019, 9, 1135.	1.9	10
67	Preparation of mesoporous CoNiO2 hexagonal nanoparticles for asymmetric supercapacitors via a hydrothermal microwave carbon bath process. New Journal of Chemistry, 2019, 43, 15066-15071.	1.4	4
68	N, S Dual-Doped Carbon Derived from Dye Sludge by Using Polymeric Flocculant as Soft Template. Nanomaterials, 2019, 9, 991.	1.9	4
69	Two-dimensional NiAl layered double oxides as non-noble metal catalysts for enhanced CO methanation performance at low temperature. Fuel, 2019, 255, 115770.	3.4	26
70	Hierarchical CoNiO2 polyhedral mesoporous nanoparticles: Hydrothermal microwave carbon bath process synthesis and ultrahigh electrochemical activity for detection of Cu(II). Electrochimica Acta, 2019, 320, 134581.	2.6	9
71	K5B19O31: A Deepâ€Ultraviolet Congruent Melting Compound. ChemistrySelect, 2019, 4, 10436-10441.	0.7	4
72	A Review of Recent Advances of Dielectric Barrier Discharge Plasma in Catalysis. Nanomaterials, 2019, 9, 1428.	1.9	73

#	Article	IF	CITATIONS
73	Highly Efficient Multifunctional Co–N–C Electrocatalysts with Synergistic Effects of Co–N Moieties and Co Metallic Nanoparticles Encapsulated in a N-Doped Carbon Matrix for Water-Splitting and Oxygen Redox Reactions. ACS Applied Materials & Interfaces, 2019, 11, 39809-39819.	4.0	80
74	Nitrogen and Sulfur Coâ€Ðoped Graphene‣ike Carbon from Industrial Dye Wastewater for Use as a Highâ€Performance Supercapacitor Electrode. Global Challenges, 2019, 3, 1900043.	1.8	17
75	A Review on the Promising Plasma-Assisted Preparation of Electrocatalysts. Nanomaterials, 2019, 9, 1436.	1.9	29
76	DBD Plasma Combined with Different Foam Metal Electrodes for CO2 Decomposition: Experimental Results and DFT Validations. Nanomaterials, 2019, 9, 1595.	1.9	13
77	Mn-Ce-Fe-Al mixed oxide nanoparticles via a high shear mixer facilitated coprecipitation method for low temperature selective catalytic reduction of NO with NH3. Applied Catalysis A: General, 2019, 586, 117237.	2.2	23
78	Effective Oxygen Reduction Reaction Performance of FeCo Alloys In Situ Anchored on Nitrogen-Doped Carbon by the Microwave-Assistant Carbon Bath Method and Subsequent Plasma Etching. Nanomaterials, 2019, 9, 1284.	1.9	19
79	Two-dimensional MnAl mixed-metal oxide nanosheets prepared via a high-shear-mixer-facilitated coprecipitation method for enhanced selective catalytic reduction of NO with NH3. Chemical Engineering and Processing: Process Intensification, 2019, 145, 107664.	1.8	10
80	A Critical Review of Recent Progress and Perspective in Practical Denitration Application. Catalysts, 2019, 9, 771.	1.6	27
81	One-step synthesis of nickel–iron layered double hydroxides with tungstate acid anions <i>via</i> flash nano-precipitation for the oxygen evolution reaction. Sustainable Energy and Fuels, 2019, 3, 237-244.	2.5	45
82	Highly active N,S co-doped hierarchical porous carbon nanospheres from green and template-free method for super capacitors and oxygen reduction reaction. Electrochimica Acta, 2019, 318, 272-280.	2.6	60
83	Cu-Doped Porous Carbon Derived from Heavy Metal-Contaminated Sewage Sludge for High-Performance Supercapacitor Electrode Materials. Nanomaterials, 2019, 9, 892.	1.9	15
84	High efficient oxygen reduction performance of Fe/Fe3C nanoparticles in situ encapsulated in nitrogen-doped carbon via a novel microwave-assisted carbon bath method. Nano Materials Science, 2019, 1, 131-136.	3.9	9
85	Highly-Dispersed Ni-NiO Nanoparticles Anchored on an SiO2 Support for an Enhanced CO Methanation Performance. Catalysts, 2019, 9, 506.	1.6	77
86	Modulating surface chemistry of heteroatom-rich micropore carbon cloth electrode for aqueous 2.1â€V high-voltage window all-carbon supercapacitor. Journal of Power Sources, 2019, 431, 232-238.	4.0	35
87	Enhanced selective catalytic reduction of NO with NH3 via porous micro-spherical aggregates of Mn–Ce–Fe–Ti mixed oxide nanoparticles. Green Energy and Environment, 2019, 4, 311-321.	4.7	40
88	Enhanced Photocatalytic Degradation of Organic Dyes via Defect-Rich TiO2 Prepared by Dielectric Barrier Discharge Plasma. Nanomaterials, 2019, 9, 720.	1.9	46
89	Molecular-level design of Fe-N-C catalysts derived from Fe-dual pyridine coordination complexes for highly efficient oxygen reduction. Journal of Catalysis, 2019, 372, 245-257.	3.1	56
90	Hydrochlorination of acetylene over the Ru-based catalysts treated by plasma under different atmospheres. Plasma Science and Technology, 2019, 21, 085501.	0.7	6

#	Article	IF	CITATIONS
91	N-doped Carbon Coated CoO Nanowire Arrays Derived from Zeolitic Imidazolate Framework-67 as Binder-free Anodes for High-performance Lithium Storage. Scientific Reports, 2019, 9, 5934.	1.6	12
92	Synthesis of hierarchical Li4SiO4 nanoparticles/flakers composite from vermiculite/MCM-41 hybrid with improved CO2 capture performance under different CO2 concentrations. Chemical Engineering Journal, 2019, 371, 424-432.	6.6	20
93	Defect-Rich Nickel Nanoparticles Supported on SiC Derived from Silica Fume with Enhanced Catalytic Performance for CO Methanation. Catalysts, 2019, 9, 295.	1.6	7
94	Enhanced CO ₂ decomposition via metallic foamed electrode packed in self-cooling DBD plasma device. Plasma Science and Technology, 2019, 21, 085504.	0.7	24
95	Enhanced low-temperature catalytic carbon monoxide methanation performance <i>via</i> vermiculite-derived silicon carbide-supported nickel nanoparticles. Sustainable Energy and Fuels, 2019, 3, 965-974.	2.5	19
96	Defective ZnS nanoparticles anchored in situ on N-doped carbon as a superior oxygen reduction reaction catalyst. Journal of Energy Chemistry, 2019, 39, 152-159.	7.1	29
97	Synthesis and formation mechanism of monodisperse Mn-Co-Ni-O spinel nanocrystallines. Advanced Powder Technology, 2019, 30, 1269-1276.	2.0	6
98	Nitrogen self-doped porous carbon nanosheets derived from azo dye flocs for efficient supercapacitor electrodes. Carbon Letters, 2019, 29, 455-460.	3.3	3
99	Designed formation of NiCo2O4 with different morphologies self-assembled from nanoparticles for asymmetric supercapacitors and electrocatalysts for oxygen evolution reaction. Electrochimica Acta, 2019, 296, 719-729.	2.6	86
100	An ultralight nitrogen-doped carbon aerogel anchored by Ni-NiO nanoparticles for enhanced microwave adsorption performance. Journal of Alloys and Compounds, 2019, 776, 43-51.	2.8	54
101	Improved oxygen reduction reaction via a partially oxidized Co-CoO catalyst on N-doped carbon synthesized by a facile sand-bath method. Chinese Chemical Letters, 2019, 30, 624-629.	4.8	15
102	Highly selective catalytic reduction of NOx by MnOx–CeO2–Al2O3 catalysts prepared by self-propagating high-temperature synthesis. Journal of Environmental Sciences, 2019, 75, 124-135.	3.2	31
103	Microspherical MnO2-CeO2-Al2O3 mixed oxide for monolithic honeycomb catalyst and application in selective catalytic reduction of NOx with NH3 at 50â€~150â€~°C. Chemical Engineering Journal, 2018, 346, 182-192.	6.6	59
104	Voltammetric lidocaine sensor by using a glassy carbon electrode modified with porous carbon prepared from a MOF, and with a molecularly imprinted polymer. Mikrochimica Acta, 2018, 185, 78.	2.5	32
105	3D nitrogen-doped graphite foam@Prussian blue: an electrochemical sensing platform for highly sensitive determination of H2O2 and glucose. Mikrochimica Acta, 2018, 185, 86.	2.5	28
106	Nitrogen and Sulfur Self-Doped Activated Carbon Directly Derived from Elm Flower for High-Performance Supercapacitors. ACS Omega, 2018, 3, 4724-4732.	1.6	122
107	Heteroatom-doped porous carbon from methyl orange dye wastewater for oxygen reduction. Green Energy and Environment, 2018, 3, 172-178.	4.7	39
108	Facile synthesis of hollow MnFe2O4 nanoboxes based on galvanic replacement reaction for fast and sensitive VOCs sensor. Sensors and Actuators B: Chemical, 2018, 258, 589-596.	4.0	34

#	Article	IF	CITATIONS
109	High-efficiency removal of NO _x using dielectric barrier discharge nonthermal plasma with water as an outer electrode. Plasma Science and Technology, 2018, 20, 014020.	0.7	16
110	Ultralow-weight loading Ni catalyst supported on two-dimensional vermiculite for carbon monoxide methanation. Chinese Journal of Chemical Engineering, 2018, 26, 1873-1878.	1.7	25
111	N-Doping of plasma exfoliated graphene oxide <i>via</i> dielectric barrier discharge plasma treatment for the oxygen reduction reaction. Journal of Materials Chemistry A, 2018, 6, 2011-2017.	5.2	94
112	pH-responsive chitosan-based flocculant for precise dye flocculation control and the recycling of textile dyeing effluents. RSC Advances, 2018, 8, 39334-39340.	1.7	20
113	Atmospheric-Pressure Cold Plasma Activating Au/P25 for CO Oxidation: Effect of Working Gas. Nanomaterials, 2018, 8, 742.	1.9	16
114	Design of an Extended Experiment with Electrical Double Layer Capacitors: Electrochemical Energy Storage Devices in Green Chemistry. Sustainability, 2018, 10, 3630.	1.6	14
115	High CO Methanation Performance of Two-Dimensional Ni/MgAl Layered Double Oxide with Enhanced Oxygen Vacancies via Flash Nanoprecipitation. Catalysts, 2018, 8, 363.	1.6	30
116	Synthesis of Both Powdered and Preformed MnO <i>_x</i> –CeO ₂ –Al ₂ O ₃ Catalysts by Self-Propagating High-Temperature Synthesis for the Selective Catalytic Reduction of NO <i>_x</i> with NH ₃ . ACS Omega, 2018, 3, 5692-5703.	1.6	17
117	Scalable synthesis of the lithium silicate-based high-temperature CO2 sorbent from inexpensive raw material vermiculite. Chemical Engineering Journal, 2018, 349, 562-573.	6.6	51
118	Critical role of iron carbide nanodots on 3D graphene based nonprecious metal catalysts for enhancing oxygen reduction reaction. Electrochimica Acta, 2018, 281, 502-509.	2.6	17
119	Up-scaled flash nano-precipitation production route to develop a MnOx–CeO2–Al2O3 catalyst with enhanced activity and H2O resistant performance for NOx selective catalytic reduction with NH3. Chemical Engineering Research and Design, 2018, 134, 476-486.	2.7	23
120	Clarification of Active Sites at Interfaces between Silica Support and Nickel Active Components for Carbon Monoxide Methanation. Catalysts, 2018, 8, 293.	1.6	15
121	Methyl Chloride Synthesis over Metal Chlorides-Modified Mesoporous Alumina Catalyst. Catalysts, 2018, 8, 99.	1.6	8
122	Enhanced Low Temperature NO Reduction Performance via MnOx-Fe2O3/Vermiculite Monolithic Honeycomb Catalysts. Catalysts, 2018, 8, 100.	1.6	38
123	DBD Plasma-ZrO2 Catalytic Decomposition of CO2 at Low Temperatures. Catalysts, 2018, 8, 256.	1.6	36
124	Two-Dimensional Layered Double Hydroxides for Reactions of Methanation and Methane Reforming in C1 Chemistry. Materials, 2018, 11, 221.	1.3	32
125	Three-Dimensional Honeycomb-Like Porous Carbon with Both Interconnected Hierarchical Porosity and Nitrogen Self-Doping from Cotton Seed Husk for Supercapacitor Electrode. Nanomaterials, 2018, 8, 412.	1.9	52
126	Enhanced Oxygen Vacancies in a Two-Dimensional MnAl-Layered Double Oxide Prepared via Flash Nanoprecipitation Offers High Selective Catalytic Reduction of NOx with NH3. Nanomaterials, 2018, 8, 620.	1.9	19

#	Article	IF	CITATIONS
127	Few-layer TiO ₂ –B nanosheets with N-doped graphene nanosheets as a highly robust anode for lithium-ion batteries. RSC Advances, 2017, 7, 7864-7869.	1.7	10
128	Activated carbon supported VN, Mo 2 N, and W 2 N as catalysts for acetylene hydrochlorination. Journal of Industrial and Engineering Chemistry, 2017, 50, 72-78.	2.9	9
129	Direct decomposition of CO ₂ using selfâ€cooling dielectric barrier discharge plasma. , 2017, 7, 721-730.		19
130	Flute type micropores activated carbon from cotton stalk for high performance supercapacitors. Journal of Power Sources, 2017, 359, 88-96.	4.0	161
131	Effective Catalytic Performance of Plasma-Enhanced W2N/AC as Catalysts for Acetylene Hydrochlorination. Topics in Catalysis, 2017, 60, 1016-1023.	1.3	6
132	Highly Active and Stable ZrO ₂ -SiO ₂ -Supported Cu-Catalysts for the Hydrogenation of Dimethyl Oxalate to Methyl Glycolate. ChemistrySelect, 2017, 2, 4823-4829.	0.7	13
133	A free-standing electrochemical sensor based on graphene foam-carbon nanotube composite coupled with gold nanoparticles and its sensing application for electrochemical determination of dopamine and uric acid. Journal of Electroanalytical Chemistry, 2017, 801, 129-134.	1.9	47
134	Two-dimensional porous SiO2 nanomesh supported high dispersed Ni nanoparticles for CO methanation. Chemical Engineering Journal, 2017, 326, 774-780.	6.6	28
135	Non-stoichiometric carbon-coated LiFe _x PO ₄ as cathode materials for high-performance Li-ion batteries. RSC Advances, 2017, 7, 33544-33551.	1.7	9
136	Plasma-enhanced copper dispersion and activity performance of Cu-Ni/ZrO2 catalyst for dimethyl oxalate hydrogenation. Catalysis Communications, 2017, 102, 31-34.	1.6	14
137	An activated carbon derived from tobacco waste for use as a supercapacitor electrode material. New Carbon Materials, 2017, 32, 592-599.	2.9	98
138	Nitrogen-Doped Carbon Nanoparticles for Oxygen Reduction Prepared via a Crushing Method Involving a High Shear Mixer. Materials, 2017, 10, 1030.	1.3	16
139	Enhanced Oxygen Reduction Reaction by In Situ Anchoring Fe2N Nanoparticles on Nitrogen-Doped Pomelo Peel-Derived Carbon. Nanomaterials, 2017, 7, 404.	1.9	39
140	Effect of Different Nano-Sized Silica Sols as Supports on the Structure and Properties of Cu/SiO2 for Hydrogenation of Dimethyl Oxalate. Catalysts, 2017, 7, 75.	1.6	11
141	Two-Dimensional Layered Double Hydroxide Derived from Vermiculite Waste Water Supported Highly Dispersed Ni Nanoparticles for CO Methanation. Catalysts, 2017, 7, 79.	1.6	19
142	Environmental Benign Synthesis of Lithium Silicates and Mg-Al Layered Double Hydroxide from Vermiculite Mineral for CO2 Capture. Catalysts, 2017, 7, 105.	1.6	21
143	Activated Carbon Supported Mo-Ti-N Binary Transition Metal Nitride as Catalyst for Acetylene Hydrochlorination. Catalysts, 2017, 7, 200.	1.6	8
144	Nitrogen-Doped Banana Peel–Derived Porous Carbon Foam as Binder-Free Electrode for Supercapacitors. Nanomaterials, 2016, 6, 18.	1.9	65

#	Article	IF	CITATIONS
145	Nickel catalysts supported on amino-functionalized MCM-41 for syngas methanation. RSC Advances, 2016, 6, 66957-66962.	1.7	21
146	Synthesis of mesoporous TiO ₂ @C@MnO ₂ multi-shelled hollow nanospheres with high rate capability and stability for lithium-ion batteries. RSC Advances, 2016, 6, 65243-65251.	1.7	14
147	Molecularly imprinted polymer functionalized nanoporous Au-Ag alloy microrod: Novel supportless electrochemical platform for ultrasensitive and selective sensing of metronidazole. Electrochimica Acta, 2016, 208, 10-16.	2.6	38
148	A green adsorbent derived from banana peel for highly effective removal of heavy metal ions from water. RSC Advances, 2016, 6, 45041-45048.	1.7	96
149	Effect of Pd Doping on the Cu ⁰ /Cu ⁺ Ratio of Cu-Pd/SiO ₂ Catalysts for Ethylene Glycol Synthesis from Dimethyl Oxalate. ChemistrySelect, 2016, 1, 2857-2863.	0.7	19
150	Synthesis and characterization of alkali metal molybdates with high catalytic activity for dye degradation. RSC Advances, 2016, 6, 54553-54563.	1.7	15
151	Fabrication of ultra-sensitive and selective dopamine electrochemical sensor based on molecularly imprinted polymer modified graphene@carbon nanotube foam. Electrochemistry Communications, 2016, 64, 42-45.	2.3	65
152	Hybridization of graphene nanosheets and carbon-coated hollow Fe ₃ O ₄ nanoparticles as a high-performance anode material for lithium-ion batteries. Journal of Materials Chemistry A, 2016, 4, 2453-2460.	5.2	128
153	Glucose-assisted hydrothermal synthesis of few-layer reduced graphene oxide wrapped mesoporous TiO ₂ submicrospheres with enhanced electrochemical performance for lithium-ion batteries. RSC Advances, 2016, 6, 20741-20749.	1.7	10
154	High efficient nickel/vermiculite catalyst prepared via microwave irradiation-assisted synthesis for carbon monoxide methanation. Fuel, 2016, 171, 263-269.	3.4	44
155	Metal organic frameworks derived porous lithium iron phosphate with continuous nitrogen-doped carbon networks for lithium ion batteries. Journal of Power Sources, 2016, 304, 42-50.	4.0	46
156	Two-Dimensional Porous Silica Nanomesh from Expanded Multilayered Vermiculite via Mixed Acid Leaching. Nanoscience and Nanotechnology Letters, 2016, 8, 1028-1032.	0.4	10
157	Effect of Au nano-particle aggregation on the deactivation of the AuCl3/AC catalyst for acetylene hydrochlorination. Scientific Reports, 2015, 5, 10553.	1.6	30
158	Three-dimensional flower-like Co(OH)2 microspheres of nanoflakes/nanorods assembled on nickel foam as binder-free electrodes for High performance supercapacitors. Materials Letters, 2015, 158, 17-20.	1.3	19
159	Controllable synthesis of nano-sized LiFePO 4 /C via a high shear mixer facilitated hydrothermal method for high rate Li-ion batteries. Electrochimica Acta, 2015, 173, 448-457.	2.6	56
160	Hydrochlorination of acetylene using expanded multilayered vermiculite (EML-VMT)-supported catalysts. Chinese Chemical Letters, 2015, 26, 1101-1104.	4.8	11
161	Application of mesoporous carbon nitride as a support for an Au catalyst for acetylene hydrochlorination. Chemical Engineering Science, 2015, 135, 472-478.	1.9	35
162	Phosphotungstic Acid Supported on Mesoporous Graphitic Carbon Nitride as Catalyst for Oxidative Desulfurization of Fuel. Industrial & Engineering Chemistry Research, 2015, 54, 2040-2047.	1.8	114

#	Article	IF	CITATIONS
163	Applications of graphene and related nanomaterials in analytical chemistry. New Journal of Chemistry, 2015, 39, 2380-2395.	1.4	69
164	Development of a Heterogeneous Non-Mercury Catalyst for Acetylene Hydrochlorination. ACS Catalysis, 2015, 5, 5306-5316.	5.5	105
165	Novel Electrochemical Sensing Platform Based on a Molecularly Imprinted Polymer Decorated 3D Nanoporous Nickel Skeleton for Ultrasensitive and Selective Determination of Metronidazole. ACS Applied Materials & Interfaces, 2015, 7, 15474-15480.	4.0	75
166	Hollow palladium–copper bimetallic nanospheres with high oxygen reduction activity. Electrochimica Acta, 2015, 176, 222-229.	2.6	22
167	Upâ€5caled Microspherical Aggregates of LiFe _{0.4} V _{0.4} PO ₄ /C Nanocomposites as Cathode Materials for Highâ€Rate Liâ€Ion Batteries. Energy Technology, 2015, 3, 496-502.	1.8	5
168	LiFePO ₄ nanoparticles growth with preferential (010) face modulated by Tween-80. RSC Advances, 2015, 5, 9745-9751.	1.7	56
169	Electrochemical determination of trace lead(II) with enhanced sensitivity and selectivity by three-dimensional nanoporous gold leaf and self-assembled homocysteine monolayer. Journal of Electroanalytical Chemistry, 2015, 758, 78-84.	1.9	19
170	Boron and Nitrogen Codoped Carbon Layers of LiFePO ₄ Improve the High-Rate Electrochemical Performance for Lithium Ion Batteries. ACS Applied Materials & Interfaces, 2015, 7, 20134-20143.	4.0	85
171	Application of a H ₄ SiMo ₁₂ O ₄₀ @SiO ₂ catalyst with a hollow core–shell structure to oxidative desulfurization. RSC Advances, 2015, 5, 76182-76189.	1.7	15
172	Two-dimensional SnS ₂ @PANI nanoplates with high capacity and excellent stability for lithium-ion batteries. Journal of Materials Chemistry A, 2015, 3, 3659-3666.	5.2	126
173	High Electrochemical Performance of LiFePO4 Cathode Material via In-Situ Microwave Exfoliated Graphene Oxide. Electrochimica Acta, 2015, 151, 240-248.	2.6	42
174	High-performance lithium iron phosphate with phosphorus-doped carbon layers for lithium ion batteries. Journal of Materials Chemistry A, 2015, 3, 2043-2049.	5.2	78
175	Fabrication of highly sensitive and selective electrochemical sensor by using optimized molecularly imprinted polymers on multi-walled carbon nanotubes for metronidazole measurement. Sensors and Actuators B: Chemical, 2015, 206, 647-652.	4.0	111
176	Overwhelming microwave irradiation assisted synthesis of olivine-structured LiMPO4 (M=Fe, Mn, Co) Tj ETQq0 0	0 rgBT /O	verlock 10 Tf
177	Optimized electrochemical performance of three-dimensional porous LiFePO4/C microspheres via microwave irradiation assisted synthesis. Journal of Power Sources, 2014, 271, 223-230.	4.0	45
178	Mechanism studies of LiFePO ₄ cathode material: lithiation/delithiation process, electrochemical modification and synthetic reaction. RSC Advances, 2014, 4, 54576-54602.	1.7	44
179	Nitrogenâ€Doped Pitchâ€Based Spherical Active Carbon as a Nonmetal Catalyst for Acetylene Hydrochlorination. ChemCatChem, 2014, 6, 2339-2344.	1.8	55
180	High-Purity Fe ₃ S ₄ Greigite Microcrystals for Magnetic and Electrochemical Performance. Chemistry of Materials, 2014, 26, 5821-5829.	3.2	97

#	ARTICLE	IF	CITATIONS
181	MOF-templated formation of porous CuO hollow octahedra for lithium-ion battery anode materials. Journal of Materials Chemistry A, 2013, 1, 11126.	5.2	361
182	Disposable electrochemical immunosensor for simultaneous assay of a panel of breast cancer tumor markers. Analyst, The, 2012, 137, 4727.	1.7	36
183	Electrochemical capacitive properties of CNT fibers spun from vertically aligned CNT arrays. Journal of Solid State Electrochemistry, 2012, 16, 1775-1780.	1.2	52
184	Electrochemical biosensor based on graphene oxide–Au nanoclusters composites for l-cysteine analysis. Biosensors and Bioelectronics, 2012, 31, 49-54.	5.3	205
185	Three-Dimensional Porous LiFePO4: Design, Architectures and High Performance for Lithium Ion Batteries. Current Inorganic Chemistry, 2012, 2, 194-212.	0.2	39
186	Fluorescence resonance energy transfer sensor between quantum dot donors and neutral red acceptors and its detection of BSA in micelles. Dyes and Pigments, 2011, 91, 304-308.	2.0	29
187	Layer-by-layer self-assembly CdTe quantum dots and molecularly imprinted polymers modified chemiluminescence sensor for deltamethrin detection. Sensors and Actuators B: Chemical, 2011, 156, 222-227.	4.0	55
188	Preparation and electrochemical performance of Li3V2(PO4)3/C cathode material by spray-drying and carbothermal method. Journal of Solid State Electrochemistry, 2010, 14, 883-888.	1.2	35
189	Porous micro-spherical aggregates of LiFePO4/C nanocomposites: A novel and simple template-free concept and synthesis via sol–gel-spray drying method. Journal of Power Sources, 2010, 195, 6873-6878.	4.0	100
190	Up-scalable synthesis, structure and charge storage properties of porous microspheres of LiFePO4@C nanocomposites. Journal of Materials Chemistry, 2009, 19, 9121.	6.7	89
191	Preparation and characterization of mesoporous LiFePO4/C microsphere by spray drying assisted template method. Journal of Power Sources, 2009, 189, 794-797.	4.0	84
192	Reaction mechanism and electrochemical performance of LiFePO4/C cathode materials synthesized by carbothermal method. Electrochimica Acta, 2009, 54, 7389-7395.	2.6	59
193	Facile Template-Free Synthesis and Characterization of Elliptic α-Fe2O3 Superstructures. Journal of Physical Chemistry C, 2009, 113, 8092-8096.	1.5	51
194	Synthesis and Performance of Cathode Material Li ₃ V ₂ (PO ₄) ₃ / by Spray Drying and Carbothermal Method (SDATM). Wuji Cailiao Xuebao/Journal of Inorganic Materials, 2009, 24, 349-352.	С _{0.6}	2
195	Bal3O9OH: A new alkaline-earth metal hydroxy iodates with two groups. New Journal of Chemistry, 0, ,	1.4	1